Smectic-C Order, In-Plane Domains, and Nematic Reentrance in a Microscopic Model of Liquid Crystals

Roland R. Netz and A. Nihat Berker

Department of Physics, Massachusetts Institute of Technology, Cambridge, Massachusetts 02139

(Received 26 August 1991)

A microscopic model of liquid crystals, with frustrated dipolar, van der Waals, and benzene-ring steric hindrance interactions, yields reentrant phase diagrams with the sequence nematic–smectic-A_d–nematic–smectic-A_1–smectic-C. The Lindemann criterion of melting is adapted to liquid crystals and Monte Carlo simulation is used. The smectic-A_1 and -C phases occur in two versions, one pointing to in-plane domain formation. Layer tilting is found to be due to permeation-rotation lock-in. The model yields three types of smectic-C phases distinguished by tilt saturation.

PACS numbers: 64.70.Md, 05.70.Fh, 61.30.By, 82.60.Fa

Experiments on polar liquid crystals have yielded strikingly rich phase diagrams exhibiting nematic reentrance phenomena and a diversity of smectic phases distinguished by layer structures and tilting [1–4]. Most of these effects have until now not received a microscopic theoretical explanation. In the work reported here, the frustrated spin-gas model, previously used to explain reentrance [5,6], is substantially developed. Intermolecular van der Waals interactions and steric hindrances due to core benzene-ring aspect ratios are included, in addition to frustrated dipolar interactions, yielding qualitatively new effects: (1) Smectic-C phases are obtained, with the layer tilting resulting from a permeation-rotation lock-in. This microscopic model yields three types of smectic-C phases distinguished by tilt saturation [7]. (2) The smectic-A_1 and -C phases occur in two versions, based on the competition between dipolar and van der Waals interactions, one version pointing to in-plane domain formation. The microscopic mechanism for reentrance becomes apparent in terms of the interpenetrating coexistence of order and disorder. Thus, the connected microscopic mechanisms for tilting, domains, and reentrance are revealed. Phase diagram trends, as well as calculated specific heats, layer thicknesses, tilt angles, and dimer concentrations, are in agreement with experiments. The calculations are done by Monte Carlo sampling. We have adapted the Lindemann criterion for melting to obtain the phase diagrams.

The model consists of molecules that occupy n consecutive sites, along the z direction, on a three-dimensional stacked triangular lattice. The triangular arrangement normal to the molecular axes reflects the close packing of actual liquid crystals. Positional fluctuations in the x-y plane away from the triangular arrangement have been investigated and found not to cause or affect reentrance phenomena [5]. This property of lateral fluctuations was subsequently confirmed by x-ray-scattering experiments [3]. Positional fluctuations along the z direction (permeations) are important and are included. The discrete positioning along the z axis has a physical basis. It reflects the preferred mutual permeation positions of neighboring molecules. This molecular corrugation, incorporated as the n segments, may be caused, depending on chemical structure, either by core benzene rings or tail carbon atoms.

Each molecule interacts with its six in-plane nearest-neighbor molecules: (1) Each molecule has a dipole, in the current study located at its end segment and pointing along the molecular axis. The dipole-dipole interaction is

$$V_d(\mathbf{r},\hat{\mathbf{s}}_1,\hat{\mathbf{s}}_2)=B[\hat{\mathbf{s}}_1\cdot\hat{\mathbf{s}}_2-3(\hat{\mathbf{s}}_1\cdot\hat{\mathbf{r}})(\hat{\mathbf{s}}_2\cdot\hat{\mathbf{r}})]/r^3,$$

where $\mathbf{r}$ is the separation of dipoles with orientations given by the unit vectors $\hat{\mathbf{s}}_1$ and $\hat{\mathbf{s}}_2$, and $\hat{\mathbf{r}}=\mathbf{r}/|\mathbf{r}|$. Because of the liquid close packing reflected by the in-plane triangular arrangement, the orientational degrees of freedom (up or down dipole) are frustrated for many permeational configurations. (2) Each of the n molecular segments has a van der Waals interaction with any nearest-neighbor-positioned segment of another molecule, via $V_w(a)=4\varepsilon[(\sigma/a)^{12}-(\sigma/a)^6]$, where a is the separation between the segments. Consistently with the latter potential, we take the length of a molecule to be $l=n\sigma$ and the discrete permeation positions to be separated by σ. (3) The benzene rings in the cores cause an in-plane molecular aspect ratio. The width of a benzene ring is 6.8 Å, whereas the typical intermolecular separations are between 4.8 and 5.5 Å. Accordingly, in our model, the larger transverse width of a molecule points between pairs of nearest neighbors and is subject to a variable amount of steric interference. This is accounted for by augmenting, by a factor of $\Gamma_1\approx 1.2$, the intermolecular interaction of a pair that, sterically optimally, has the large transverse widths parallel to each other and normal to the intermolecular separation. If the large transverse widths are parallel to each other, but, less optimally, tilt toward the intermolecular separation, the intermolecular interaction is augmented by a factor $\Gamma_2\approx 1.1$. This is an accounting of the fact that in regimes of our model where rotational correlations are important, the intermolecular interactions of dominant configurations are monotonically increasing, in absolute value, with decreasing lateral separation, and sterically less hindered molecules pack

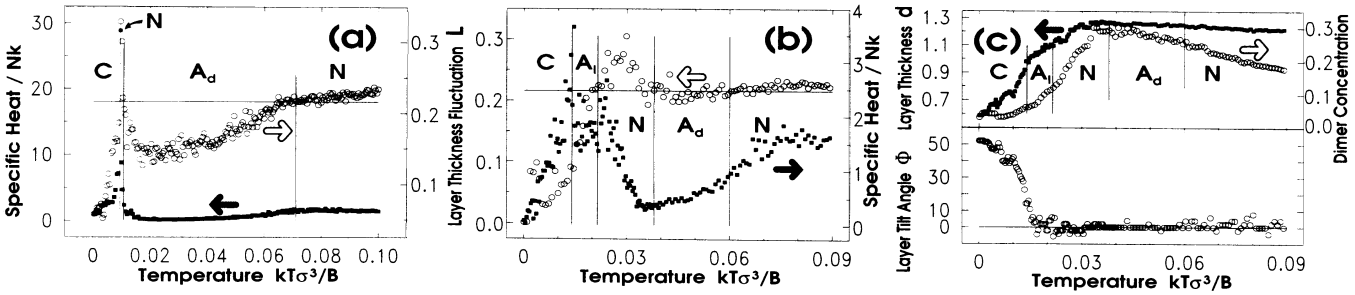

FIG. 1. Specific heat and layer-thickness fluctuation L along the dashed line at (a) $a/l=0.19714$ and (b) $a/l=0.19557$ in the phase diagram of Fig. 2(a). Note the high-temperature singularity occurring in (a) at the layer-thickness fluctuation of $L=0.2157$, which establishes the Lindemann criterion for this compound, confirmed by the low-temperature specific-heat signals. (c) Other calculations along $a/l=0.19557$. The layer thickness $d=(l+\langle\delta\rangle)\cos\phi$ is normalized to the smectic-A_1 phase. The molecular dimer concentration is the fraction of nearest-neighbor dipoles that point oppositely and have the same z coordinate.

closer. However, for benzene-ring steric hindrance to be effective, the molecular pair must be in a congested environment. Thus, the steric factors mentioned above are used only for pairs in which a given molecule overlaps by at least n_0 segments with the nearest neighbors in opposite directions. Finally, when this overlap condition is satisfied, the intermolecular interaction of the pairs not mentioned above is augmented by a factor $\Gamma_3\approx 1.05$. The latter specification was necessary only to obtain the experimentally observed relative specific heats of the various transitions [8]. This is an empirical indication of the nonlinearity of the induced dipoles underlying the van der Waals interaction.

Rather than using the approximate mapping of the previous studies, the partition function of the model was calculated by Monte Carlo sampling. We considered $N=24\times 24$ molecules that have a nearest-neighbor overlap of at least one segment, imbedded and evolving in the three-dimensional lattice. This is a study of a cross section of bulk material if vertical interactions are negligible. We have developed a new Lindemann criterion that determines the nematic-smectic transition, in terms of the layer thickness fluctuation due to the molecular positions along the z direction: $L=\langle(\delta-\langle\delta\rangle)^2\rangle^{1/2}/l$, where $\langle\rangle$ denotes averaging over Monte Carlo samplings and $\delta=\langle\langle(z_i-z_j)^2\rangle\rangle^{1/2}$, with $\langle\langle\rangle\rangle$ denoting averaging over the system and z_i and z_j coordinates of nearest-neighbor molecules. A singularity in L [e.g., high-temperature side of Fig. 1(a)] establishes the criterion for the nematic-smectic transition of a given compound ($B/\sigma^3\varepsilon$, n, n_0, and Γ_i values), which is confirmed by specific-heat signals [e.g., low-temperature sides of Figs. 1(a) and 1(b)]. This singularity occurs typically for L between 0.15 and 0.25. The smectic-C phase boundaries, on the other hand, are determined by the onset of layer tilt [e.g., Fig. 1(c)]. The individual molecules have discrete positional (along the z direction), orientational (dipole up or down), and rotational (threefold) degrees of freedom. For each data point, typically between 10000 and 20000 Monte Carlo trials per molecule were taken, after discarding 1000 trials per molecule. At each trial, a molecule was allowed to sample its entire permeation range and, in a certain

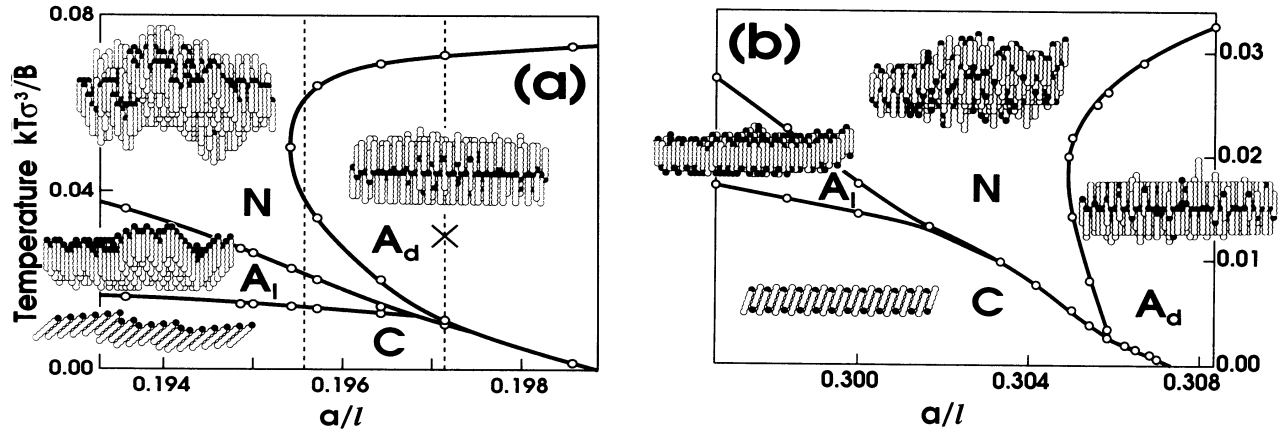

FIG. 2. Calculated phase diagrams for (a) a strongly dipolar system ($B\sigma^3/\varepsilon=14.29$) with $n=7$, $n_0=10$, $\Gamma_1=1.20$, $\Gamma_2=1.10$, and $\Gamma_3=1.05$; and (b) a less strongly dipolar system ($B\sigma^3/\varepsilon=4$) with $n=6$, $n_0=9$, $\Gamma_1=1.120$, $\Gamma_2=1.050$, and $\Gamma_3=1.035$. The horizontal axes give the ratio of the lateral molecular separation a to molecular length l. The separation a should be monotonically decreasing with pressure (or mixture concentration). The insets are global molecular configurations occurring in each of the phases.

fraction f of trials, its orientational ($f=0.5$) and rotational (f between 0.1 and 0.5) degrees of freedom.

Figure 2 shows phase diagrams evaluated for different dipole strengths. The insets are actual global molecular configurations found in each phase. Figure 3(c) shows that, in the smectic-A_d phase, more than one-third of the molecules freely permeate within a microscopic range and reverse their dipoles (reflecting the distribution in the statistical ensemble). These molecules provide the local filling necessary to relieve the frustration of the remaining molecules: The latter are no longer close packed and can therefore correlate orientationally and permeationally, in turn fixing the microscopic permeation range of the former set of molecules [Fig. 3(c)]. Thus, because of this interpenetrating coexistence of order and disorder, the smectic-A_d phase has substantial amounts of both gained entropy and lowered energy.

Dipolar frustration can also be relieved by optimizing the combined energies of all neighboring molecules, resulting in the correlated permeation of triplets as shown in Figs. 3(a) and 3(b), which occur respectively for strong and less strong dipolar interactions relative to van der Waals interactions. The smectic-A_1 phases are dominated by these triplets. The choices of the inequivalent pairings in triplets across the system give respectively the entropy of the ground states of the Ising antiferromagnet on the triangular lattice and of the three-state Potts antiferromagnet on the Kagomé lattice, which are less than the entropy of the smectic-A_d phase which is over $\ln(2n)/3$ per molecule. Accordingly, the smectic-A_1 phases are expected and found at lower temperatures than the smectic-A_d phase. The intervening nematic phase is due to the competition and cancellation of the two types of smectic correlations [6]. In actual liquid crystals, these entropy considerations should not be quantitatively modified much, when given in fuzzy versions, by the relaxation of the lattice constraint.

The triplets dominating the smectic-A_1 phases are tilted [Figs. 3(a) and 3(b)]. However, local tilt does not automatically imply global tilt. The latter happens at temperatures where the energy differences due to steric hindrances become important. All pair energies in Figs. 3(a) and 3(b) are favorable (negative), being most favorable for the pairs shown with the double lines. Therefore, energy is minimized by the rotational states shown in the top views in Figs. 3(a) and 3(b). We thus find that the tilts of individual triplets, due to dipolar interactions, are coordinated to neighboring triplets by the aspect ratio of shared molecules. Note that in Fig. 3(b) the degeneracy is not totally lifted: only every other pair of adjacent triplets can be energetically optimized, leading to similarly oriented molecules forming lines that freely meander along only two in-plane directions and thereby creating an average tilt, as seen in the inset. As the system is cooled, when essentially all possible triplets are in the energetically optimal states, the tilt angles saturate at respectively $\tan^{-1}(2\sigma/a)$ or $\tan^{-1}(\sigma/2a)$, where a is the lateral intermolecular separation. These would correspond to saturation angles that would cluster around 50° or 20°, respectively. Furthermore, according to our microscopic picture, molecules that are not effectively corrugated will not show tilt saturation, yielding a third group of smectic-C behavior [7].

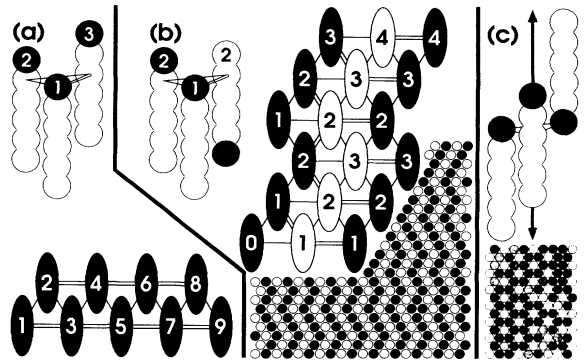

FIG. 3. Nearest-neighbor triplet configurations that dominate, respectively, the two smectic-A_1 phases and the smectic-A_d phase. In the latter, one molecule is free to permeate. The numerals indicate the z coordinates. The double line indicates the most favorable pair (dipolar and van der Waals) interaction in the triplet. In (a) and (b), top views of the layers dominated by these triplets are also shown, with the molecular aspect ratios. Optimizing the steric packing of the most favorable interaction introduces tilt propagation, as seen by the z coordinates. Bottom of (b): The most favorable interaction can be sterically optimized only in every other pair of adjacent triplets, leading to similarly oriented molecules forming lines that freely meander along only two in-plane directions. The net tilt is, thus, from right to left. Bottom of (c): Top view of a portion of the layer in the smectic-A_d phase, calculated for $kT\sigma^3/B=0.03$ and $a/l=0.19714$ in the phase diagram of Fig. 2(a) (marked there by a cross). The black and white molecules remained positionally and orientationally (respectively in opposite directions) fixed over fifty Monte Carlo samplings per molecule in the entire system. The gray molecules permeated and flipped their orientations, as indicated by the tone of grayness.

In the global phase diagram of our model system, the low-temperature smectic phases, A_1 and C, appear in two separate and distinct versions, as seen in the insets of Figs. 2(a) and 2(b) and corresponding to Figs. 3(a) and 3(b). In the physical systems, the molecules are structurally up-down asymmetric. Thus, the oriented versions of the smectic-A_1 and -C phases will develop local curvature. Global curvature would imply the loss of layer sliding entropy, so that the layer will tend to form in-plane orientational domain boundaries, reversing its local curvature and thereby avoiding global curvature. These oriented (therefore indicative of in-plane domain formation) versions of the smectic-A_1 and -C phases occur, in our calculations, for strongly dipolar molecules [Fig. 2(a)], whereas the nonoriented versions occur for less strongly dipolar molecules [Fig. 2(b)], in agreement with

experiments [2,4]. The above indication of in-plane domain formation due to local curvature is valid for thermotropic systems. In lyotropic systems, where maintaining a sliding entropy of packed layers is not an issue due to the intervening water molecules, local curvature controlled by this dipolar–van der Waals competition should influence the formation of micelles and lamellar phases.

We are very grateful to P. Cladis, C. W. Garland, and G. Nounesis for many useful discussions. Support by an Evangelisches Studienwerk Fellowship is gratefully acknowledged by R.R.N. This research was supported by NSF Grant No. DMR-90-22933 and by JSEP Contract No. DAAL 03-89-C0001.

[1] P. E. Cladis, Phys. Rev. Lett. **35**, 48 (1975).

[2] F. Hardouin, A. M. Levelut, M. F. Achard, and G. Sigaud, J. Chim. Phys. **80**, 53 (1983).

[3] A. R. Kortan, H. von Känel, R. J. Birgeneau, and J. D. Litster, J. Phys. (Paris) **45**, 529 (1984).

[4] N. H. Tinh, Mol. Cryst. Liq. Cryst. **127**, 143 (1985).

[5] A. N. Berker and J. S. Walker, Phys. Rev. Lett. **47**, 1469 (1981).

[6] J. O. Indekeu and A. N. Berker, Phys. Rev. A **33**, 1158 (1986).

[7] A categorization that is quite similar was deduced, from then available experimental data, by A. de Vries, in *Liquid Crystals*, edited by F. D. Seva (Marcel Dekker, New York, 1979), pp. 1–72, but appears not to have been addressed in the subsequent experimental literature.

[8] J. O. Indekeu, A. N. Berker, C. Chiang, and C. W. Garland, Phys. Rev. A **35**, 1371 (1987).

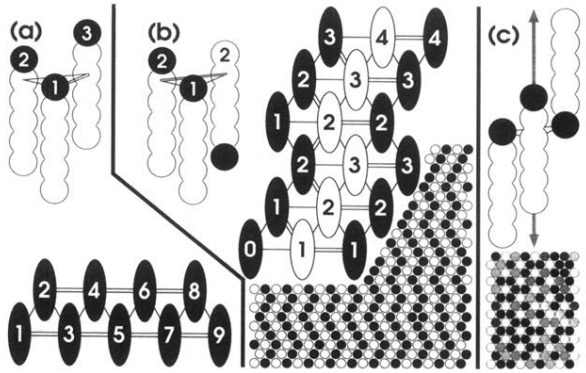

FIG. 3. Nearest-neighbor triplet configurations that dominate, respectively, the two smectic-A_1 phases and the smectic-A_d phase. In the latter, one molecule is free to permeate. The numerals indicate the z coordinates. The double line indicates the most favorable pair (dipolar and van der Waals) interaction in the triplet. In (a) and (b), top views of the layers dominated by these triplets are also shown, with the molecular aspect ratios. Optimizing the steric packing of the most favorable interaction introduces tilt propagation, as seen by the z coordinates. Bottom of (b): The most favorable interaction can be sterically optimized only in every other pair of adjacent triplets, leading to similarly oriented molecules forming lines that freely meander along only two in-plane directions. The net tilt is, thus, from right to left. Bottom of (c): Top view of a portion of the layer in the smectic-A_d phase, calculated for $kT\sigma^3/B=0.03$ and $a/l=0.19714$ in the phase diagram of Fig. 2(a) (marked there by a cross). The black and white molecules remained positionally and orientationally (respectively in opposite directions) fixed over fifty Monte Carlo samplings per molecule in the entire system. The gray molecules permeated and flipped their orientations, as indicated by the tone of grayness.